

# DOGMA: Weaving Structural Information into Data-centric Single-cell Transcriptomics Analysis

Ru Zhang<sup>1</sup> Xunkai Li<sup>1</sup> Yaxin Deng<sup>1</sup> Sicheng Liu<sup>1</sup> Daohan Su<sup>1</sup> Qiangqiang Dai<sup>1</sup> Hongchao Qin<sup>1</sup>  
Rong-Hua Li<sup>1</sup> Guoren Wang<sup>1</sup> Jia Li<sup>2</sup>

## Abstract

Recently, data-centric AI methodology has been a dominant paradigm in single-cell transcriptomics analysis, which treats data representation rather than model complexity as the fundamental bottleneck. In the review of current studies, earlier sequence methods treat cells as independent entities and adapt prevalent ML models to analyze their directly inherited sequence data. Despite their simplicity and intuition, these methods overlook the latent intercellular relationships driven by the functional mechanisms of biological systems and the inherent quality issues of the raw sequence data. Therefore, a series of structured methods has emerged. Although they employ various heuristic rules to capture intricate intercellular relationships and enhance the raw sequencing data, these methods often neglect biological prior knowledge. This omission incurs substantial overhead and yields suboptimal graph representations, thereby hindering the utility of ML models.

To address them, we propose DOGMA, a holistic data-centric framework designed for the structural reshaping and semantic enhancement of raw data through multi-level biological prior knowledge. Transcending reliance on stochastic heuristics, DOGMA redefines graph construction by integrating Statistical Anchors with Cell Ontology and Phylogenetic Trees to enable deterministic structure discovery and robust cross-species alignment. Furthermore, Gene Ontology is utilized to bridge the feature-level semantic gap by incorporating functional priors. In complex multi-species and multi-organ benchmarks, DOGMA achieves SOTA performance, exhibiting superior zero-shot robustness and sample efficiency while operating

with significantly lower computational cost.

## 1. Introduction

Elucidating cellular functional characteristics and their complex collaborative mechanisms lies at the heart of understanding biological systems (Regev et al., 2017). Breakthroughs in single-cell RNA sequencing (scRNA-seq) technologies have revolutionized this exploration by enabling the quantification of genome-wide expression at single-cell resolution (Macosko et al., 2015; Zheng et al., 2017). In response to these burgeoning analytical demands, the field of single-cell analysis is undergoing a profound paradigm shift: moving from a “Model-Centric” approach, which blindly pursues architectural complexity, to a “Data-Centric” paradigm that prioritizes data quality and structural representation (Zha et al., 2023).

This paradigm shift reveals a key insight: as deep learning architectures mature, the performance bottleneck in representation learning often stems not from insufficient Model Capacity, but from the quality and structural integrity of the input data (Zha et al., 2023). For raw single-cell sequencing data, this bottleneck manifests in two aspects: First, the raw data suffers from significant intrinsic imperfections, including high dimensionality, extreme sparsity, and inevitable technical noise (e.g., dropout events) (Kharchenko et al., 2014; Luecken & Theis, 2019); Second, cells are not isolated entities but reside within complex biological networks. While inherent biological functional correlations exist between cells, raw data often lacks an explicit representation of these associations.

Failure to fundamentally address these issues means that merely expanding neural network depth will not only encounter diminishing marginal returns but also risk overfitting statistical artifacts, leading the model to learn spurious biological correlations. Therefore, constructing a unified Data-Centric framework capable of simultaneously achieving data denoising and structural reshaping has become an urgent imperative. Regrettably, however, existing mainstream methods, whether structure-agnostic sequence-based modeling (Yang et al., 2022; Theodoris et al., 2023; Cui

<sup>1</sup>Department of Computer Science, Beijing Institute of Technology, Beijing, China <sup>2</sup>The Hong Kong University of Science and Technology (GZ), Guangzhou, China. Correspondence to: Rong-Hua Li <lironghuabit@126.com>.

et al., 2024) or current noise-constrained graph construction approaches (Wen et al., 2022; Buterez et al., 2022; Cao et al., 2024), have failed to effectively address this dual challenge.

Sequence-based architectures (e.g., Transformers (Yang et al., 2022; Cui et al., 2024)), owing to their intuitive appeal, have emerged as the dominant paradigm in early exploratory studies. Drawing inspiration from Natural Language Processing (NLP), these methodologies analogize cells to documents and treat sequencing data as tokens, attempting to capture latent biological patterns through large-scale pre-training (Theodoris et al., 2023; Cui et al., 2024).

However, as illustrated in Figure 1 (Left), this analogy encounters dual limitations within the biological context. First, while documents are typically treated as independent samples, cells are not isolated entities but reside within intricate collaborative networks. Sequence-based methods impose an independent and identically distributed (i.i.d.) assumption on the data, thereby severing the intrinsic topological correlations between cells (Battaglia et al., 2018). Second, these approaches naively inherit the intrinsic imperfections of raw sequencing data, including high-dimensional sparsity and technical noise (Luecken & Theis, 2019). The absence of explicit denoising mechanisms at the input level renders these models highly susceptible to data quality bottlenecks.

This strategy of fitting complex models to low-quality data explains why large-scale models like scGPT (Cui et al., 2024), despite consuming immense computational resources, often fail to outperform simple generative baselines (e.g., scVI (Lopez et al., 2018)) in zero-shot tasks (Kedzierska et al., 2025). Attempting to force sequence models to implicitly fit scRNA-seq data is a high-cost, low-efficiency strategy, compelling models to memorize technical noise rather than capturing biological patterns. As shown in Figure 1(a), empirical study confirms that blindly scaling model size cannot compensate for the absence of explicit structural priors: the Cell Token Transformer utilizes 3.5M parameters yet lags behind the structure-aware GNN, which achieves superior accuracy with only one-third of parameters.

**Conclusion:** Sequence-Based data representation could not effectively capture cellular network structures.

**Remark:** *Although simple and intuitive, this modeling perspective treats cells as isolated individuals, ignoring the intrinsic biological associations between cells.*

While structured approaches attempt to mitigate the limitations of sequence models by incorporating graph structures, the graphs they construct suffer from fundamental defects in two core dimensions: topological connectivity and node features, thereby limiting their effectiveness.

First, at the level of topological structure, the cellular connections constructed by existing methods are often riddled

with errors and lack a systematic biological perspective. In heterogeneous graphs (e.g., scMoGNN (Wen et al., 2022), scGNN (Wang et al., 2021)), introduced housekeeping gene nodes evolve into “super hubs,” artificially bridging distinct cells and smoothing out specific differences (Li et al., 2018). As quantified in Figure 1(b), these high-degree hubs precipitate an explosive growth in edge density and memory consumption, imposing severe computational bottlenecks without yielding proportional performance gains.

Meanwhile, methods relying on statistical distance (e.g., k-NN (Wolf et al., 2018; Buterez et al., 2022)) are susceptible to being misled by batch effects, resulting in the construction of spurious neighborhood relationships (Haghverdi et al., 2018). Even prior works attempting to incorporate prior knowledge into graph construction are typically confined to microscopic molecular-level associations (Cao et al., 2024; Yang et al., 2023), lacking a hierarchical and systematic global reference coordinate system such as Cell Ontology (Diehl et al., 2016). This approach to graph construction, utilizing only fragmented biological constraints, struggles to macroscopically correct the pervasive global biases within the data, failing to establish a truly robust cellular topological structure.

Second, at the level of node features, existing methods perform only shallow mathematical compression, lacking the capacity for biologically meaningful interpretation. Most existing graph construction methods solely employ HVG or PCA processed data to build their topology (Luecken & Theis, 2019; Stuart et al., 2019); however, this essentially amounts to mere statistical compression of numerical values. Without incorporating external knowledge bases like Gene Ontology (The Gene Ontology Consortium, 2021) to provide explicit biological definitions, downstream models struggle to comprehend the specific functional significance represented by these compressed values. In the absence of such biological functional semantic annotations, downstream models treat biological signals and technical noise indistinguishably. Consequently, the learned representations are highly susceptible to noise interference, rendering them unable to precisely lock onto critical biological features.

**Conclusion:** Existing graph construction methods could not build robust cellular topological networks.

**Remark:** *Heterogeneous graphs smooth out biological differences, while homogeneous graphs are misled by data noise. They lack the global knowledge prior.*

To bridge this semantic gap, we introduce **DOGMA** (Deterministic Ontology-Guided Modeling Approach). This data-centric framework reformulates graph construction from unverified statistical inference to knowledge-anchored structure discovery. Unlike methods relying solely on stochastic heuristics, DOGMA injects multi-level symbolic priors to regularize the structure learning process.

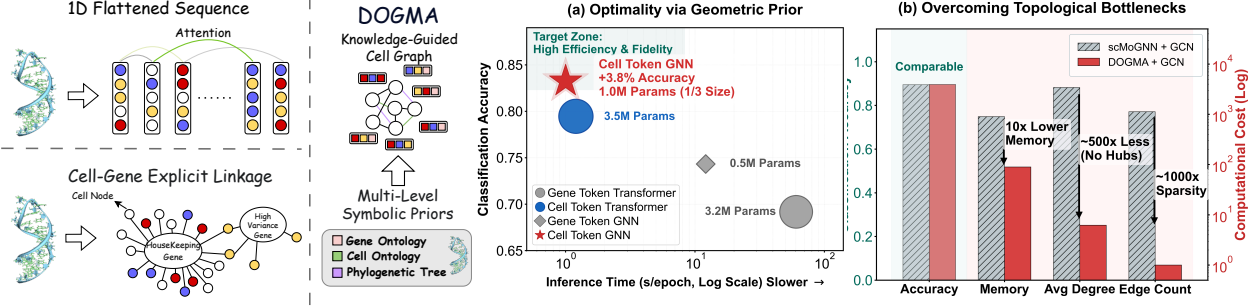


**Figure 1. DOGMA: A Data-Centric Paradigm Shift.** (Left) Data structure of current input paradigms. Sequence-based inputs lose topological structure, while heterogeneous graphs suffer from structural redundancy. (Middle) DOGMA acts as a universal structure inference engine. It injects multi-level knowledge (Gene Ontology, Cell Ontology, Phylogeny) to produce a knowledge-guided cell graph. (Right) Empirical validation. (a) GNN achieves the Target Zone (High Efficiency & High Performance) with significantly fewer parameters than Transformers. (b) DOGMA overcomes topological bottlenecks, reducing memory usage by 10x compared to scMoGNN while maintaining competitive accuracy.

Specifically, we construct a composite cell topology jointly constrained by statistical alignment and multilayer prior knowledge:

- (1) **Statistical Anchors:** MNN is employed for initial batch-invariant alignment;
- (2) **Hierarchical Constraints:** The Cell Ontology is integrated to enforce biological relatedness;
- (3) **Evolutionary Context:** Phylogenetic Trees is incorporated to capture cross-species lineage conservation.

Furthermore, we leverage the Gene Ontology for feature-level data enhancement.

Empirically, we validate the effectiveness of DOGMA through extensive experiments. By aligning cells via universal biological knowledge, DOGMA establishes a robust and scalable structural foundation for the next generation of single-cell analysis.

Our main contributions are summarized as follows:

**New Perspective:** We champion a data-centric paradigm shift, transitioning from metric-based heuristics to deterministic, ontology-guided structure discovery. We establish that a knowledge-anchored cell topology serves as a robust structural foundation, effectively transcending the limitations imposed by the inherent noise of raw sequencing data.

**Benchmark Dataset:** Beyond methodology, we curate and release a comprehensive multi-dimensional graph benchmark. Constructed via our scalable DOGMA pipeline, this suite encompasses diverse biological axes, including cross-species and cross-organ regimes. Our benchmark provides deterministic, knowledge-anchored topologies, serving as a rigorous testbed for evaluating topological robustness and zero-shot transferability across complex domain shifts.

**SOTA Performance:** Extensive experiments demonstrate that DOGMA consistently outperforms baselines, exhibiting exceptional robustness in zero-shot generalization and data-scarce scenarios. Notably, it achieves these gains while operating with orders-of-magnitude lower computational

overhead than large-scale models, empirically validating the principle that prioritizing data structural quality yields greater returns than resource-intensive parameter scaling.

## 2. Preliminaries

In this section, we formally define the single-cell data structures, the external symbolic knowledge bases, and the core research problem of knowledge-guided structure discovery.

**Data Definition.** Let  $\mathcal{C} = \{c_1, \dots, c_N\}$  denote a set of  $N$  single cells and  $G = \{g_1, \dots, g_M\}$  denote a set of  $M$  genes. The raw input consists of two components: (1) A gene expression matrix  $\mathbf{X} \in \mathbb{R}^{N \times M}$ , where the row vector  $\mathbf{x}_i \in \mathbb{R}^M$  represents the gene expression profile of cell  $c_i$ ; and (2) Associated metadata, where each cell  $c_i$  is annotated with a species domain label  $s_i \in \mathcal{S}$ . Crucially, we distinguish between a reference set where the cell type label  $y_i$  is provided, and a query set where  $y_i$  remains unknown. Based on these inputs, our fundamental objective is to infer a robust adjacency matrix  $\mathbf{A} \in \{0, 1\}^{N \times N}$  that captures intrinsic biological connectivity and transcend noise-induced artifacts, serving as the topological backbone for the following graph representation learning.

**Symbolic Knowledge Definition.** To mitigate the inherent noise and sparsity in raw sequencing data, we leverage multi-level structured biological priors: (1) *Cell Ontology (CO)*: We define the Cell Ontology as a Directed Acyclic Graph (DAG)  $\mathcal{G}_{CO} = (\mathcal{V}_{CO}, \mathcal{E}_{CO})$ , where nodes  $\mathcal{V}_{CO}$  represent standardized cell types and edges  $\mathcal{E}_{CO}$  represent hierarchical relationships. For reference cells, the labels serve as direct indices  $y_i \in \mathcal{V}_{CO}$ . (2) *Gene Ontology (GO)*: We define the Gene Ontology as a DAG  $\mathcal{G}_{GO} = (\mathcal{V}_{GO}, \mathcal{E}_{GO})$ , where nodes represent gene functional terms. The mapping between genes and functions is provided by the GO database: for each gene feature  $g_j \in G$ , its associated func-

tional terms correspond to a subset of nodes  $\mathcal{V}_{g_j} \subset \mathcal{V}_{GO}$ . (3) *Phylogeny*: We model cross-species evolutionary relationships via a phylogenetic tree  $\mathcal{T}_{phy} = (\mathcal{V}_{phy}, \mathcal{E}_{phy})$ . The species labels  $s_i$  correspond to leaf nodes in this tree, where the tree distance  $d_{phy}(\cdot, \cdot)$  reflects evolutionary divergence.

**Problem Formulation.** Standard paradigms typically construct an adjacency matrix  $\mathbf{A}_{naive}$  based on metric heuristics in the feature space (e.g.,  $k$ -NN). However, due to technical noise,  $\mathbf{A}_{naive}$  often fails to reflect the true biological topology. To strictly prevent target label leakage, we formulate knowledge-guided structure discovery as a two-stage process distinguishing between labeled reference data  $\mathcal{C}_{ref}$  and unlabeled query data  $\mathcal{C}_{query}$ : (1) *Base Graph Construction*: Using the reference data  $\mathbf{X}_{ref}$  and full metadata  $\{y_i, s_i\}_{ref}$ , alongside knowledge bases  $\{\mathcal{G}_{CO}, \mathcal{G}_{GO}, \mathcal{T}_{phy}\}$ , we construct a high-quality Homogeneous Cell Graph  $\mathcal{G}^* = (\mathcal{C}_{ref}, \mathcal{E}^*)$ . Here, the edge set  $\mathcal{E}^*$  is determined by biological semantic consistency rather than solely by statistical correlation. (2) *Inductive Graph Mapping*: Based on  $\mathcal{G}^*$ , we aim to learn an encoder  $f_\theta$  that maps query cells  $\mathcal{C}_{query}$  to the latent space  $\mathbf{Z} \in \mathbb{R}^{N \times d}$  solely using their expression  $\mathbf{X}_{query}$  and species  $s_i$ , without accessing their ground-truth labels  $y_i$ .

### 3. Related Work

**Deep Paradigms:** The field has transitioned from statistical approaches to deep architectures. Recently, Large Transcriptome Models like scBERT (Yang et al., 2022) and scGPT (Cui et al., 2024) have adapted Transformer architectures, treating gene expression profiles as “sentences.” While scalable, this tokenization requires massive pre-training to learn purely statistical patterns, leading to high data inefficiency without biological grounding. Conversely, Graph Neural Networks (e.g., scGNN (Wang et al., 2021)) offer biologically plausible inductive biases by modeling cellular interactions, yet their efficacy is strictly bounded by the quality of the input graph structure.

**Evolution of Graph Construction Strategies.** Current graph construction paradigms largely rely on data-driven heuristics, lacking external verification. (1) *Metric-based Heuristics*: Dominant approaches like SPRING (Weinreb et al., 2018) and scGAC (Cheng & Ma, 2022) construct  $k$ -NN graphs based on Euclidean or correlation metrics. These methods rely on the assumption that geometric proximity equals biological relatedness, rendering them vulnerable to stochastic noise and technical batch effects (Luecken & Theis, 2019). Moreover, lacking a shared semantic coordinate system, these methods are typically limited to *transductive* settings, failing to generalize to unseen batches or cell types. (2) *Latent-Graph Learning*: Methods like CellVGAE (Buterez et al., 2022) and scBiGNN (Yang et al., 2023) infer graph structures within learned latent spaces.

While they improve upon raw features, the inferred topology often overfits to the internal statistical consistency of the training data rather than true biological fidelity, limiting cross-dataset transferability (Rosen et al., 2024). (3) *Heterogeneous Modeling*: Approaches like scMoGNN (Wen et al., 2022) explicitly link cells and genes. However, high-degree gene nodes act as “super-hubs,” leading to severe information over-smoothing (Li et al., 2018) and prohibitive memory overheads.

**Knowledge-Informed Representation Learning.** A growing body of work seeks to integrate biological priors. *Statistical Alignment*: Methods like scGCN (Song et al., 2021) utilize Mutual Nearest Neighbors (MNN) (Haghverdi et al., 2018) to align distributions. However, MNN is a statistical heuristic reliant on local geometry, lacking semantic verification. *Architectural Constraints*: Recent approaches like expiMap (Lotfollahi et al., 2023) directly embed Gene Ontology into the neural network architecture. These methods represent a *model-centric* approach, where knowledge is hard-coded as architectural constraints for interpretability.

**Our Distinction:** In contrast to these *model-centric* architectures, DOGMA adopts a *data-centric* paradigm. We focus on engineering the input topology itself rather than the model architecture. By rigorously combining statistical anchors with symbolic priors (Cell Ontology & Phylogeny), we construct a universal, biologically verified graph structure. This allows DOGMA to be used as a universal plug-and-play graph module for any standard GNN backbone, distinguishing our contribution from specialized end-to-end architectures.

### 4. Methods

We propose **DOGMA** (Deterministic Ontology-Guided Modeling Approach), a holistic data-centric framework that bridges the gap between noisy statistical observations and biologically grounded truths. Unlike conventional methods that blindly fit data artifacts, DOGMA operates through a calibrated pipeline: it first initializes a statistical manifold from raw data, then rectifies the topology via deterministic biological masking, and finally enforces semantic consistency through dual-view feature fusion.

#### 4.1. Data Pipeline and Feature Initialization

**Preprocessing Pipeline:** We standardize raw single-cell transcriptomic data from CellXGene through a rigorous abstraction process to generate robust model inputs:

**Quality Control (QC):** We apply strict filtering to mitigate technical noise, removing genes expressed in fewer than 3 cells and filtering cells based on mitochondrial content ( $> 5\%$ ) and extreme read counts ( $5^{\text{th}}\text{--}95^{\text{th}}$  percentiles).

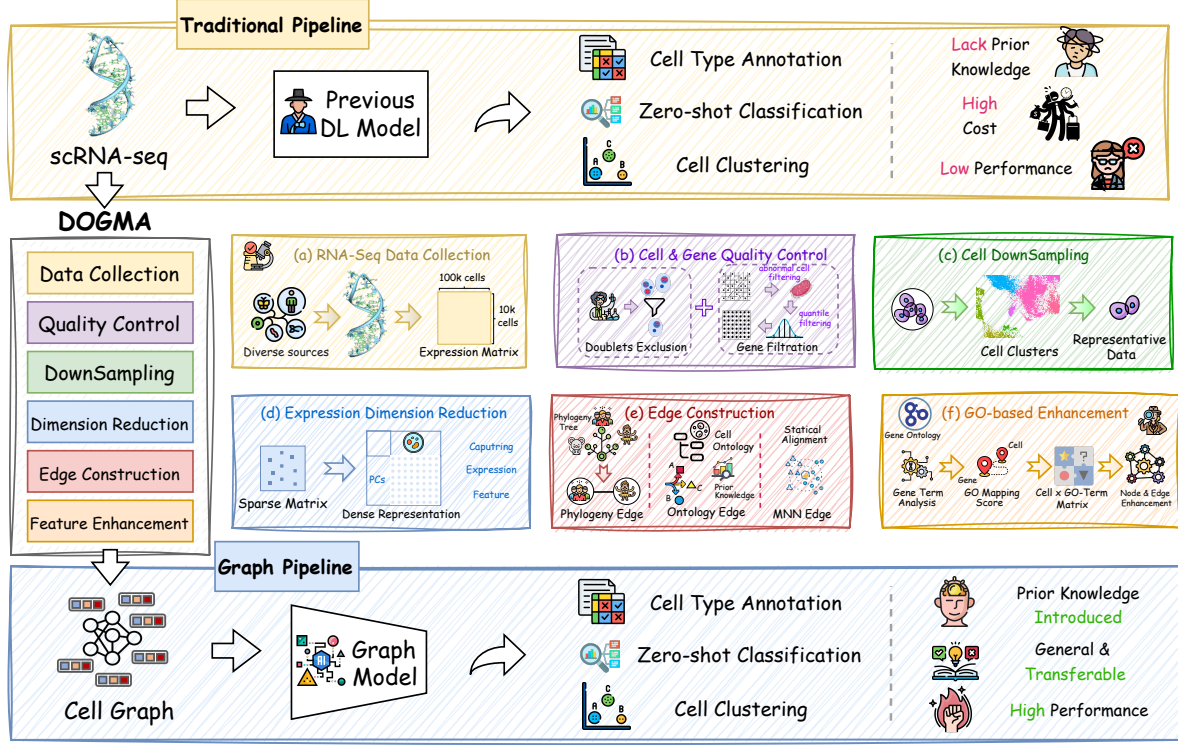


**Figure 2. The DOGMA Framework (Top)** Traditional pipelines rely on black-box models that lack prior knowledge, leading to high computational costs and suboptimal performance. **(Middle)** Our proposed data-centric workflow transforms raw scRNA-seq data into a knowledge-guided cell graph through six stages: (a-b) rigorous data curation and quality control; (c-d) representative downsampling and dimensionality reduction; (e) deterministic topology construction integrating Phylogeny, Cell Ontology, and MNN edges; and (f) feature enhancement via Gene Ontology (GO). **(Bottom)** The resulting Cell Graph serves as a universal, interpretable input for Graph Models, enabling high-performance, transferable analysis across zero-shot and clustering tasks.

**Stratified Downsampling:** To balance computational tractability with biological diversity, we employ stratified downsampling. This ensures the retention of rare cell populations, preventing class imbalance from biasing the subsequent topology inference.

**Feature Initialization:** While we acknowledge the semantic limitations of Principal Component Analysis (PCA), it remains effective for capturing dominant variance. We project the log-normalized expression matrix into a dense feature space  $\mathbf{X} \in \mathbb{R}^{N \times 50}$ .

**Benchmark Datasets.** We curated a multi-tier benchmark suite evaluating robustness across increasing levels of biological complexity: **Level 1: Brain** (Cross-Species, Single-Organ), **Level 2: Human** (Single-Species, Multi-Organ), and **Level 3: Multi** (Cross-Species, Multi-Organ).

## 4.2. Deterministic Topology Rectification

The core of DOGMA is to derive a robust adjacency matrix  $\mathbf{A}$  by filtering the noisy statistical manifold through deterministic biological lenses. We define the final edge set  $\mathcal{E}$  as the union of three complementary sub-graphs:

$$\mathcal{E} = \mathcal{E}_{\text{Align}} \cup \mathcal{E}_{\text{Onto}} \cup \mathcal{E}_{\text{Phy}}$$

### 1. Technical Alignment Layer ( $\mathcal{E}_{\text{Align}}$ ).

Before introducing biological priors, we must correct for domain-specific technical artifacts (e.g., batch effects). We employ Mutual Nearest Neighbors (MNN) as a *technical alignment* step. We employ Mutual Nearest Neighbors (MNN) to enforce reciprocity, ensuring edges exist only if cells from distinct domains identify each other as neighbors, thereby correcting distributional shifts.

### 2. Ontology-Guided Semantic Masking ( $\mathcal{E}_{\text{Onto}}$ ).

To eliminate spurious connections caused by statistical coincidences, we impose the Cell Ontology (CO) graph as a deterministic filter. Crucially, to strictly prevent label leakage, access to cell type labels is confined exclusively to the training set. We propose a Masked Top-K strategy. For cell  $i$ , we first define a Semantic Mask  $\mathcal{M}_i$  that activates only for biologically plausible candidates (cells with label distance  $d_{\text{CO}}(L_i, L_j) \leq 1$ ). We then search for neighbors

**Table 1. Main Performance Benchmark.** Comparison of Cell Type Annotation (Acc), Development Stage Identification (Acc), and Metadata Annotation (Acc) across different biological datasets. **Red** and **Blue** denote the best and second-best result.

Method	Cell Type (Acc)			Dev Stage (Acc)			Metadata (Acc)		
	Brain	Human	Multi	Brain	Human	Multi	Brain	Human	Multi
k-NN + GCN	0.8558	0.8488	0.8408	0.8034	0.7297	0.7432	0.7917	0.7992	.8007
k-NN + GAT	0.8127	0.8613	0.8584	0.7228	0.7565	0.7997	0.7079	0.8235	0.8730
MNN + GCN	0.8539	0.8623	0.9058	0.7996	0.8350	0.8242	0.7804	0.8300	0.8828
MNN + GAT	0.8277	0.8605	0.9155	0.7697	0.8332	<b>0.8482</b>	0.7402	0.8418	0.9048
scMoGNN + GCN	0.8390	0.8493	0.8120	0.8539	0.8448	0.7554	0.8155	<b>0.9150</b>	0.8647
scMoGNN + GAT	0.8596	0.8251	0.8137	<b>0.8858</b>	0.7238	0.7360	0.8460	<b>0.8868</b>	0.8653
scPriorGraph + GCN	0.8049	0.7663	0.7211	0.8015	0.5326	0.6920	0.7860	0.6729	0.8086
scPriorGraph + GAT	0.8086	0.7663	0.7263	0.8071	0.5299	0.6926	0.7864	0.6717	0.8097
scGPT	<b>0.9195</b>	0.8574	0.8811	<b>0.8895</b>	0.8189	0.8103	<b>0.8591</b>	0.8457	0.9037
<b>DOGMA + GCN</b>	0.8558	<b>0.8685</b>	<b>0.9195</b>	0.8277	<b>0.8555</b>	0.8168	0.8104	0.8730	<b>0.9125</b>
<b>DOGMA + GAT</b>	<b>0.8989</b>	<b>0.8730</b>	<b>0.9222</b>	0.8708	<b>0.8457</b>	<b>0.8790</b>	<b>0.8476</b>	0.8688	<b>0.9222</b>

solely within this valid semantic subspace:

$$\mathcal{N}_i^{\text{Onto}} = \text{Top-K}_{j \in \mathcal{V}} \left( \frac{\mathbf{x}_i \cdot \mathbf{x}_j}{\|\mathbf{x}_i\| \|\mathbf{x}_j\|} \odot \mathcal{M}_{ij} \right). \quad (1)$$

This mechanism ensures that edges are statistically similar only if they are first biologically validated, effectively pruning false positives inherent in raw data.

### 3. Phylogenetically Stratified Connection ( $\mathcal{E}_{\text{Phy}}$ ).

To robustly model cross-species conservation, we move beyond simple pair-wise matching by introducing a hierarchical stratification based on the Phylogenetic Tree  $\mathcal{T}$ . We compute the evolutionary distance  $\text{dist}_{\mathcal{T}}(S_a, S_b)$  between species on  $\mathcal{T}$ . Based on these distances, we define hierarchical strata and construct a compatibility matrix  $\mathbf{P}$ . Connections are permitted only between species pairs within a predefined evolutionary radius  $\delta$ , i.e.,  $\text{dist}_{\mathcal{T}}(S_i, S_j) \leq \delta$ . This prevents long-range noise where distinct species might exhibit coincidental statistical similarity due to batch effects.

### 4.3. Dual-View Semantic Fusion

To resolve the semantic gap of statistical features, we perform knowledge-aware augmentation via Gene Ontology (GO), creating a dual-view representation.

**Knowledge View (Z):** We select  $D_{go} = 200$  high-variance GO terms. For each cell, we compute a Z-score normalized enrichment vector  $\mathbf{z}_i$ , which aggregates noisy gene counts into robust functional pathway signals.

**Observation View (X):** The PCA-based statistical features capturing data-driven variance. The final node representation  $\mathbf{H}_i = [\mathbf{x}_i \parallel \mathbf{z}_i]$  fuses these orthogonal views:  $\mathbf{x}_i$  provides high-resolution variation, while  $\mathbf{z}_i$  provides robust semantic anchors. Furthermore, we explicitly construct edge features  $\mathbf{e}_{ij} = [\mathbf{H}_i \parallel \mathbf{H}_j]$  to model the *communicative context* between cells, guiding the message-passing mechanism to be context-aware.

## 5. Experiments

To validate the superiority of DOGMA, we conduct comprehensive experiments across datasets of varying biological complexity. We aim to answer the following four core questions: **Q1:** Does DOGMA establish SOTA performance in both supervised (classification) and unsupervised (clustering) representation learning tasks? **Q2:** Can DOGMA leverage biological priors to achieve robust zero-shot generalization in unseen cross-domain scenarios? **Q3:** Is DOGMA resilient to data scale variations, particularly in data-scarce regimes? **Q4:** Does DOGMA achieve a practical time-accuracy trade-off?

### 5.1. Supervised and unsupervised Performance

To answer **Q1**, we conduct systematic evaluations under two distinct learning paradigms: supervised annotation and unsupervised clustering. We compare DOGMA with four categories of baselines: naive graph methods, heterogeneous graph networks (scMoGNN), prior-driven methods (scPrior-Graph), and single-cell foundation models (scGPT).

Table 1 demonstrates the robust performance of DOGMA in supervised scenarios, where DOGMA+GAT outperforms all baselines across the vast majority of tasks. Compared to heterogeneous and prior-driven graph methods, DOGMA benefits from holistic deterministic topology construction, effectively circumventing interference from noise and sparse priors. Compared to scGPT, DOGMA achieves superior generalization in complex cross-species scenarios by introducing explicit topological structures (e.g., Multi dataset: 0.9201 vs. 0.8537). Notably, even in unsupervised clustering tasks (Table 2), DOGMA demonstrates remarkable capability in capturing intrinsic biological patterns, with ARI metrics significantly surpassing scGPT and scMoGNN. This highlights the efficacy of structural optimization over sheer model complexity.

**Table 2. Zero-shot and Clustering Benchmark.** Comparison of Cell Type Annotation (Accuracy) and Clustering (ARI & AMI) across Brain, Human, and Multi datasets. Baselines use Leiden for clustering. **Red** and **Blue** denote the best and second-best results.

Method	Zero-shot Identification(Acc)			Clustering					
	Cell Type			Brain		Human		Multi	
	Brain	Human	Multi	ARI	AMI	ARI	AMI	ARI	AMI
scGPT	<b>0.5447</b>	<b>0.4296</b>	<b>0.5064</b>	—	—	—	—	—	—
scPriorGraph	0.3255	0.3849	0.4942	0.4993	0.6449	0.4240	0.6952	<b>0.4851</b>	<b>0.7102</b>
scMoGNN	0.4494	0.3046	0.3667	<b>0.5590</b>	<b>0.7065</b>	<b>0.4347</b>	<b>0.7478</b>	0.3799	0.6982
<b>DOGMA</b>	<b>0.6039</b>	<b>0.5565</b>	<b>0.5184</b>	<b>0.4996</b>	<b>0.6594</b>	<b>0.4636</b>	<b>0.7524</b>	<b>0.5686</b>	<b>0.7740</b>

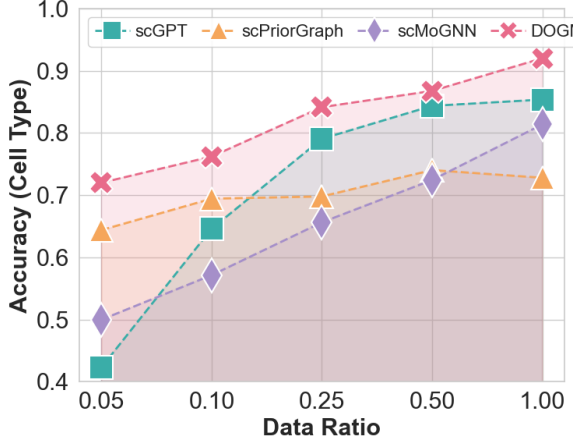


**Figure 3. Data Efficiency Analysis (Q3).** Performance comparison under varying training ratios on the Multi dataset. DOGMA (Red) maintains high accuracy even in data-scarce regimes, demonstrating superior sample efficiency compared to scPriorGraph, scMoGNN and scGPT

## 5.2. Zero-shot Generalization

To answer **Q2**, we evaluate zero-shot generalization by applying models trained on source tissues directly to unseen target domains without fine-tuning. Table 2 highlights DOGMA’s adaptability in traversing biological domains, where it consistently outperforms existing methods across cross-tissue and cross-species settings. Compared to scGPT, which suffers from severe performance degradation due to domain shifts (e.g., dropping to 0.4296 on Human), DOGMA maintains superior robustness (0.5565). This advantage stems from its reliance on universal biological priors, which serve as stable semantic anchors against distributional shifts.

## 5.3. Data Efficiency and Scaling Law

To answer **Q3**, we systematically investigate the dependency of model performance on data scale by varying the pre-training data ratio from 5% to 100% on the Multi dataset. As shown in Figure 3, DOGMA consistently outperforms baselines across all data splits, maintaining a significant lead

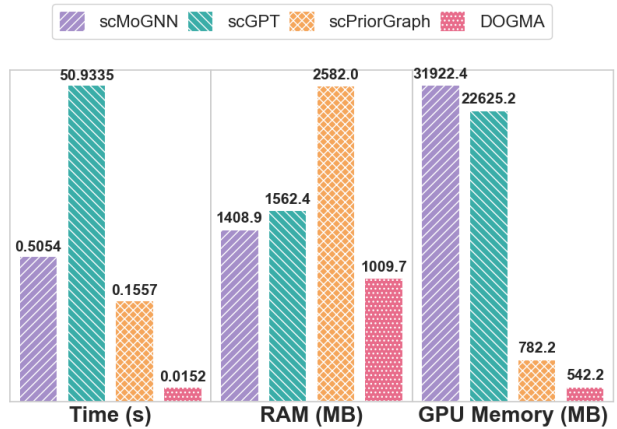


**Figure 4. Computational Efficiency Analysis (Q4).** Comparison of inference time, RAM usage, and GPU memory consumption. DOGMA operates with significantly lower resource overhead, achieving both accuracy and efficiency.

even with increasing data volume.

A striking disparity is observed in the extreme *data-scarce* regime: with only 5% of training data, DOGMA demonstrates remarkable robustness, maintaining a classification accuracy of approximately 0.72, whereas the sequence-based scGPT suffers from severe cold-start difficulties, with performance plummeting to around 0.42. Unlike scGPT which struggles in low-data regimes due to lack of priors, DOGMA’s ontology constraints enable robust reasoning with minimal data.

## 5.4. Efficiency Analysis and Resource Overhead

To address **Q4**, we benchmark computational efficiency across two critical dimensions: memory footprint and inference latency. Figure 4 reveals the substantial advantage of DOGMA over baseline models.

In terms of GPU memory, scMoGNN and scGPT consume prohibitive amounts of resources, restricting their deployment. In contrast, DOGMA achieves a remarkable 98% reduction in memory usage. Regarding inference latency,

**Table 3. Ablation Study.** Impact of different biological priors on model performance across Cell Metadata Annotation (Acc), Zero-shot Identification (Acc), and Clustering (ARI). The values represent the best performance between GCN and GAT backbones. **Bold** denotes the best result in each column.

Method	Cell Metadata (Acc)			Zero-shot Identification (Acc)			Clustering (ARI)		
	Brain	Human	Multi	Brain	Human	Multi	Brain	Human	Multi
w/o Gene Ontology	0.8076	0.8727	0.9044	0.4836	0.4426	0.4049	0.4006	0.4428	0.5510
w/o Cell Ontology	0.8113	0.8575	0.9207	0.4954	0.4192	0.3938	0.2597	0.4097	0.5278
w/o Phylogeny/Organ	0.8179	0.8613	0.9201	0.5042	0.4585	0.3868	0.3935	0.4623	0.5594
w/o All Priors	0.8165	0.8623	0.9155	0.4905	0.4157	0.3939	0.2900	0.3873	0.4341
<b>DOGMA (Full)</b>	<b>0.8989</b>	<b>0.8730</b>	<b>0.9222</b>	<b>0.6039</b>	<b>0.5565</b>	<b>0.5184</b>	<b>0.4996</b>	<b>0.4636</b>	<b>0.5686</b>

**Table 4. Case Study:** Cross-Species Semantic Alignment. Quantitative comparison of alignment stability between Raw Gene Expression and DOGMA’s GO-based Semantic Scores. Pearson correlation ( $r$ ) is measured across matched cell types between species. DOGMA demonstrates significantly higher correlation and lower variance. **Bold** denotes superior performance.

Representation Strategy	Correlation Metrics		Stability & Robustness	
	Pearson ( $r$ )	Performance Gain	Variance Reduction	Consistency (Types)
Raw Gene Expression	$0.842 \pm 0.096$	—	—	Baseline
<b>GO Pathway Scores (DOGMA)</b>	<b><math>0.986 \pm 0.007</math></b>	<b>+17.2%</b>	<b>93%</b>	<b>100% (13/13)</b>

DOGMA achieves millisecond-level inference, representing a  $>3000\times$  speedup compared to scGPT.

This efficiency stems from DOGMA’s deterministic graph construction, which avoids the heavy computational overhead of large-scale pre-training or dense heuristic graph learning.

### 5.5. Ablation Study

To address **Q3**, we conduct ablation studies isolating core components of DOGMA, as shown in Table 3. We evaluate three critical variations and their impact on supervised, zero-shot, and clustering tasks. Disabling the Cell Ontology leads to a catastrophic collapse in unsupervised clustering performance, confirming the necessity of deterministic ontology for maintaining inter-class separability in the latent space. Removing phylogenetic/organ constraints significantly impairs zero-shot identification in complex scenarios, indicating that evolutionary hierarchical constraints are central to achieving cross-species alignment. Compared to removing single components, removing all priors generally yields the most severe performance degradation. This confirms that DOGMA’s components are not merely additive but form a complementary synergy: Gene Ontology enhances feature semantics, while Cell Ontology and Phylogeny jointly construct a robust topological structure.

### 5.6. Case Study

Our case study demonstrates that DOGMA significantly mitigates inter-species expression discrepancies by projecting raw expression profiles into the Gene Ontology (GO) semantic space. As presented in Table 4, empirical data re-

veals that, in contrast to the substantial volatility observed in raw gene expression ( $r = 0.842 \pm 0.096$ ), the GO-based semantic features generated by DOGMA achieve near-perfect cross-species alignment ( $r = 0.986 \pm 0.007$ ) in all 13 cell types, reducing variance by 93%. This high-level functional consistency directly translates into superior downstream performance: ablation studies confirm that removing the GO feature enhancement module precipitates the most drastic decline in zero-shot accuracy among all biological priors. This confirms that DOGMA captures conserved “semantic anchors” that mitigate statistical perturbations, enabling robust cross-domain generalization.

## 6. Conclusion

In this paper, we identify a critical bottleneck in single-cell representation learning: the prevailing reliance on expanding model complexity to compensate for the intrinsic noise and structural deficiencies of raw sequencing data. To address this, we propose **DOGMA**, a deterministic, knowledge-guided data structure. By rigorously integrating multi-level biological priors, including Gene Ontology, Cell Ontology, and Phylogenetic Trees, DOGMA effectively transforms noisy statistical observations into biologically consistent cellular networks. Extensive empirical evaluations demonstrate that DOGMA consistently outperforms state-of-the-art sequence-based and graph-based baselines across a wide spectrum of tasks. Crucially, our approach exhibits exceptional robustness in cross-species generalization and data-scarce scenarios, while achieving orders-of-magnitude improvements in computational efficiency compared to large-scale models. These

results show that incorporating explicit biological logic into the design of data structures offers a more decisive advantage than blindly scaling neural network parameters. DOGMA establishes a solid foundation for future research that synergizes symbolic domain knowledge with data-driven learning, paving the way for more reliable and interpretable single-cell analysis.

## Impact Statement

This paper presents work whose goal is to advance the field of Machine Learning. There are many potential societal consequences of our work, none which we feel must be specifically highlighted here.

## References

Battaglia, P. W., Hamrick, J. B., Bapst, V., Sanchez-Gonzalez, A., Zambaldi, V., et al. Relational inductive biases, deep learning, and graph networks. *arXiv preprint arXiv:1806.01261*, 2018.

Buterez, D., Bica, I., Tariq, I., Andrés-Terré, H., and Liò, P. CellVGAE: an unsupervised scRNA-seq analysis workflow with graph attention networks. *Bioinformatics*, 38(5):1277–1286, 2022.

Cao, X., Huang, Y.-A., You, Z.-H., Shang, X., Hu, L., Hu, P.-W., and Huang, Z.-A. scPriorGraph: constructing biosemantic cell–cell graphs with prior gene set selection for cell type identification from scRNA-seq data. *Genome Biology*, 25(1):207, 2024.

Cheng, Y. and Ma, X. scGAC: a graph attentional architecture for clustering single-cell rna-seq data. *Bioinformatics*, 38(8):2187–2193, 2022.

Cui, H., Wang, C., Maan, H., Pang, K., Li, F., Duan, N., and Wang, B. scGPT: toward building a foundation model for single-cell multi-omics using generative AI. *Nature Methods*, 21:1470–1480, 2024.

Diehl, A. D., Meehan, T. F., Bradford, Y. M., Brush, M. H., Dahdul, W. M., Dougall, D. S., He, Y., Osumi-Sutherland, D., Ruttenberg, A., Sarntivijai, S., et al. The cell ontology 2016: enhanced content, consistency, and interoperability. *Journal of Biomedical Semantics*, 7(1):1–10, 2016.

Haghverdi, L., Lun, A. T. L., Morgan, M. D., and Marioni, J. C. Batch effects in single-cell RNA-sequencing data are corrected by matching mutual nearest neighbors. *Nature Biotechnology*, 36(5):421–427, 2018.

Kedzierska, K. Z., Crawford, L., Amini, A. P., and Lu, A. X. Zero-shot evaluation reveals limitations of single-cell foundation models. *Genome Biology*, 26(1):101, 2025. doi: 10.1186/s13059-025-03574-x.

Kharchenko, P. V., Silberstein, L., and Scadden, D. T. Bayesian approach to single-cell differential expression analysis. *Nature Methods*, 11(7):740–742, 2014.

Li, Q., Han, Z., and Wu, X.-M. Deeper Insights into Graph Convolutional Networks for Semi-Supervised Learning. In *Proceedings of the Thirty-Second AAAI Conference on Artificial Intelligence (AAAI)*, pp. 3538–3545, 2018.

Lopez, R., Regier, J., Cole, M. B., Jordan, M. I., and Yosef, N. Deep generative modeling for single-cell transcriptomics. *Nature Methods*, 15(12):1053–1058, 2018.

Lotfollahi, M., Rybakov, S., Hrovatin, K., Hediyyeh-zadeh, S., Talavera-López, C., Misharin, A. V., and Theis, F. J. Biologically informed deep learning to query gene programs in single-cell atlases. *Nature Cell Biology*, 25(2):337–350, 2023.

Luecken, M. D. and Theis, F. J. Current best practices in single-cell RNA-seq analysis: a tutorial. *Molecular Systems Biology*, 15(6):e8746, 2019.

Macosko, E. Z., Basu, A., Satija, R., Nemesh, J., Shekhar, K., Goldman, M., Tirosh, I., Bialas, A. R., Kamitaki, N., Martersteck, E. M., Trombetta, J. J., Weitz, D. A., Sanes, J. R., Shalek, A. K., Regev, A., and McCarroll, S. A. Highly parallel genome-wide expression profiling of individual cells using nanoliter droplets. *Cell*, 161(5):1202–1214, 2015.

Regev, A., Teichmann, S. A., Lander, E. S., et al. The Human Cell Atlas. *eLife*, 6:e27041, 2017. doi: 10.7554/eLife.27041.

Rosen, Y., Brbić, M., Roohani, Y., Swanson, K., Li, Z., and Leskovec, J. Toward universal cell embeddings: integrating single-cell rna-seq datasets across species with SATURN. *Nature Methods*, 2024.

Song, Q., Su, J., and Zhang, W. scGCN is a graph convolutional networks algorithm for knowledge transfer in single cell omics. *Nature Communications*, 12(1):3826, 2021.

Stuart, T., Butler, A., Hoffman, P., Hafemeister, C., Papalexi, E., Mauck, 3rd, W. M., Hao, Y., Stoeckius, M., Smibert, P., and Satija, R. Comprehensive integration of single-cell data. *Cell*, 177(7):1888–1902, 2019.

The Gene Ontology Consortium. Gene Ontology resource: enriching a GOld mine. *Nucleic Acids Research*, 49(D1):D325–D334, 2021.

Theodoris, C. V., Xiao, L., Chopra, A., Chaffin, M. D., Al Sayed, Z. R., Hill, M. C., Mantineo, H., Brydon, E. M., et al. Transfer learning enables predictions in network biology. *Nature*, 618(7965):616–624, 2023.

Wang, J., Ma, A., Chang, Y., Gong, J., Jiang, Y., Qi, R., Wang, C., Yang, H., Han, Y., and Xu, D. scGNN is a novel graph neural network framework for single-cell RNA-seq analyses. *Nature Communications*, 12(1):1882, 2021.

Weinreb, C., Wolock, S., and Klein, A. M. SPRING: a kinetic interface for visualizing high dimensional single-cell expression data. *Bioinformatics*, 34(7):1246–1248, 2018.

Wen, H., Ding, J., Jin, W., Wang, Y., Xie, Y., and Tang, J. Graph neural networks for multimodal single-cell data integration. In *Proceedings of the 28th ACM SIGKDD Conference on Knowledge Discovery and Data Mining (KDD)*, pp. 4163–4173. ACM, 2022.

Wolf, F. A., Angerer, P., and Theis, F. J. SCANPY: large-scale single-cell gene expression data analysis. *Genome Biology*, 19(1):15, 2018.

Yang, F., Wang, W., Wang, F., Fang, Y., Tang, D., Huang, J., Lu, H., and Yao, J. scBERT as a large-scale pretrained deep language model for cell type annotation of single-cell RNA-seq data. *Nature Machine Intelligence*, 4(10):852–866, 2022.

Yang, R., Dai, W., Li, C., Zou, J., Wu, D., and Xiong, H. scBiGNN: Bilevel Graph Representation Learning for Cell Type Classification from Single-cell RNA sequencing data. In *NeurIPS 2023 AI for Science Workshop*, 2023.

Zha, D., Bhat, Z. P., Lai, K.-H., Yang, F., Jiang, Z., Zhong, S., and Hu, X. Data-centric artificial intelligence: A survey. *arXiv preprint arXiv:2303.10158*, 2023.

Zheng, G. X. Y., Terry, J. M., Belgrader, P., et al. Massively parallel digital transcriptional profiling of single cells. *Nature Communications*, 8:14049, 2017.

## A. Dataset Details

To comprehensively evaluate the robustness and generalization capabilities of DOGMA, we curated three distinct graph benchmarks derived from the CellxGene database. These datasets differ in biological complexity, ranging from single-organ cross-species conservation to complex multi-organ and multi-species heterogeneity. The raw gene expression matrices were processed to retain the specific subsets listed below.

### A.1. Benchmark Construction

**1. Brain Benchmark (Level 1: Cross-Species, Single-Organ)** This benchmark focuses on modeling evolutionary conservation within the brain cortex across primates and rodents. It integrates data from three major studies covering Human, Chimpanzee, Marmoset, and Mouse.

**Source 1:** *Evolution of cellular diversity in primary motor cortex of human, marmoset monkey, and mouse.* We utilized the Marmoset (non-neuron) subset containing 4,289 cells and 14,409 genes.

**Source 2:** *Transcriptional profiling of murine oligodendrocyte precursor cells across the lifespan.* This subset includes 38,807 *Mus musculus* cells with 51,727 genes.

**Source 3:** *Molecular and cellular evolution of the primate dorsolateral prefrontal cortex (dlPFC).* We integrated two high-resolution subsets: *Pan troglodytes* (158,099 cells, 23,534 genes) and *Callithrix jacchus* (149,467 cells, 28,346 genes).

**2. Human Benchmark (Level 2: Single-Species, Multi-Organ)** Derived from the *Tabula Sapiens* atlas, this benchmark evaluates the model's ability to capture tissue heterogeneity within a single species (*Homo sapiens*). It comprises three distinct organs with high-dimensional feature spaces:

**Lung:** 65,847 cells, 61,759 genes.

**Small Intestine:** 42,036 cells, 61,759 genes.

**Tongue:** 38,754 cells, 61,759 genes.

**3. Multi Benchmark (Level 3: Cross-Species, Multi-Organ)** This is the most challenging scenario, designed to test robustness against simultaneous domain shifts in species and tissue types. It aggregates data from four studies:

**Cortex (Marmoset):** Sourced from *Comparative transcriptomics reveals human-specific cortical features* (75,861 cells, 12,897 genes).

**Cortex (Macaque):** Also sourced from the Great Apes study (89,136 cells, 19,784 genes).

**Blood (Human):** Sourced from *Tabula Sapiens* (85,233 cells, 60,606 genes).

**Thymus (Mouse):** Sourced from *Single-cell multiomic analysis of thymocyte development* (29,408 cells, 15,942 genes).

## B. Empirical Experiment Settings

### B.1. Data Representation: Tokenization Strategies

To comprehensively evaluate the proposed method against prevailing paradigms, we categorize the experimental baselines into two distinct tokenization strategies: *Cell Tokenization* and *Gene Tokenization*.

#### B.1.1. CELL TOKENIZATION

- **Definition:** Each token represents a single cell  $\mathbf{c}_i \in \mathbb{R}^{d_{gene}}$ . A set of  $N$  cells forms the input sequence/graph.
- **Setup ( $N = 200$ ):** Consistent with our proposed method, we sample a mini-batch of  $N = 200$  cells per iteration. This results in a  $200 \times 200$  interaction matrix (Adjacency or Attention map) representing cell-cell similarity.

#### B.1.2. GENE TOKENIZATION

- **Definition:** Each token represents a specific gene  $\mathbf{g}_j \in \mathbb{R}^{d_{cell}}$ . The input represents the expression profile of a single cell across gene tokens.
- **Setup:**
  1. **Gene GNN ( $N = 200$ ):** To match the GNN constraints, we select the top-200 Highly Variable Genes (HVGs) to construct a  $200 \times 200$  gene regulatory graph.

2. **Gene Transformer** ( $N = All$ ): Following standard scBERT-like implementations, this baseline processes the full sequence of expressed genes (approx. 2,000+), resulting in significant computational overhead.

## B.2. Model Architectures and Complexity Analysis

We compare four distinct configurations corresponding to the data points in Figure 1(a).

**1. Cell Token GNN (Ours,  $\star$  Red Star).** **Analysis:** By leveraging the geometric prior through a dynamically learned adjacency matrix  $\mathbf{A} \in \mathbb{R}^{200 \times 200}$ , this model efficiently captures cell manifolds. With a compact dimension of 128 and shared graph weights, it achieves optimal accuracy with only 1.0M parameters and fast inference ( $10^0$  scale).

**2. Cell Token Transformer (Baseline,  $\bullet$  Blue Circle).** **Analysis:** Requires larger hidden dimension (256) and FFN (ratio=4) to approximate relationships, tripling parameters (3.5M) while maintaining similar speed ( $N = 200$ ).

**3. Gene Token GNN (Baseline,  $\diamond$  Gray Diamond).** **Analysis:** This model constructs a  $200 \times 200$  adjacency matrix representing Gene Regulatory Networks (GRNs). Since gene regulation logic is inherently more complex than cell similarity, we utilize a significantly wider network ( $d = 512$ ) to capture high-order interactions. This results in a larger model (3.2M parameters) and slightly slower inference ( $10^1$  scale) compared to the Cell Token GNN.

**4. Gene Token Transformer (Baseline,  $\bullet$  Gray Circle).** **Analysis:** Processes full sequences with  $O(N^2)$  complexity (slow  $10^2$  inference). Hidden dimension is constrained to  $d = 64$  to avoid OOM errors, yielding 0.5M parameters.

## B.3. Implementation Details

All models were implemented using PyTorch and trained on a single NVIDIA RTX 5090 GPU.

## C. Experimental Settings

### C.1. Data Preprocessing

We evaluate DOGMA on three comprehensive benchmarks constructed from the CellxGene database to assess performance across varying biological complexities. The Human Benchmark comprises lung, small intestine, and tongue tissues. Uniquely for this human-specific dataset, we adopt the Human Cell Atlas Ontology (HCAO) instead of the standard CO to provide more granular, organ-specific semantic guidance during topology construction. All datasets undergo stratified downsampling to balance class distributions and feature initialization via PCA ( $d = 50$ ) on log-normalized gene expression counts.

### C.2. Task Settings and Evaluation

Our evaluation framework spans three distinct learning paradigms. For supervised classification tasks, including cell type, tissue, and development stage prediction, we employ a stratified split of 50% training, 20% validation, and 30% testing. In zero-shot generalization scenarios, we simulate domain shifts by holding out a subset of cell types, training on 60% (seen) and evaluating on the remaining 40% (unseen). Notably, we prioritize the Graph Attention Network (GAT) backbone for zero-shot tasks, as its attention mechanism demonstrates superior capability in capturing latent semantic relations within information-sparse regimes compared to GCNs. For unsupervised clustering, we strictly utilize the Leiden algorithm for community detection on the learned graph embeddings, reporting Adjusted Rand Index (ARI) and Adjusted Mutual Information (AMI) to quantify the alignment between derived clusters and ground-truth annotations.

### C.3. Implementation Details

Models are implemented in PyTorch Geometric on an NVIDIA RTX 5090 (scGPT uses a VGPU-800 for CUDA incompatibility). Training uses AdamW (lr=0.01, decay= $5 \times 10^{-4}$ ) for 100 epochs with early stopping (patience=20)